Biomass Conv. Bioref. (2016) 6:427–433
DOI 10.1007/s13399-016-0198-6

ORIGINAL ARTICLE

The chemometric approach applied to FTIR spectral data for the analysis of lipid content in microalgae cultivated in different nitrogen sources

Amrita Difusa[1] · **K. Mohanty**[1,2] · **Vaibhav V. Goud**[1,2]

Received: 15 November 2015 / Revised: 31 December 2015 / Accepted: 7 January 2016 / Published online: 26 January 2016

Abstract Microalgae-based biofuel production has emerged as a potential sector to extend its sustainability. Corresponding to many factors imbibed, nitrogen is considered as an essential element for microalgae cultivation. Among the four studied nitrogen sources, sodium nitrate (Na) and urea (U) showed high lipid content of 35.86 ± 2.3 and 37.35 ± 0.32 %, respectively. In terms of lipid yield, the four investigated nitrogen sources are represented in preferrential order, i.e., urea > sodium nitrate > ammonium nitrate > potassium nitrate. The Fourier transform infrared spectroscopy (FTIR) fingerprint of oil recovered from *Chloromonas* species ADIITEC-III, cultivated in different nitrogen sources, were analyzed using chemometric techniques. The chemometric techniques, i.e., cluster analysis, multidimensional scaling (MDS), and a multivariate calibration of principal component analysis (PCA), were assessed to analyze the existing spectral signatures specific to the lipid-acyl chain (3000–2800 cm^{-1}) and biomolecular fingerprint region (1800–1000 cm^{-1}) in the FTIR spectrum of the sample. The study of FTIR-coupled chemometric techniques complements the response of the nitrogen sources in lipid yield and confirmed the reliability of the method.

Keywords Chemometrics · FTIR spectroscopy · *Chloromonas* species ADIITEC-III · Principal component analysis · Cluster analysis

1 Introduction

Microalgae, a recent prototype for biofuel production have grabbed worldwide attention due to its potentiality as a sustainable and environment-friendly alternative. Despite being a potential feedstock, microalgae oil production deal with hurdles in several major stages from algal cultivation to conversion of algal oil to biofuels. In addition, these processes evoked serious challenges in the commercialization of the technology with huge investment. Therefore, the microalgae-based biofuel production requires effective technological innovation to overcome the hindrance in sustainable development of the technology.

Considering the major aspects for microalgae cultivation, nitrogen is quantitatively the most important factor for growth medium affecting the biomass, growth, and lipid productivity of various microalgae [1]. The significant intent to establish microalgae-based biofuel production is involved with several methods for biomass and lipid productivity which affects the economic feasibility of the system [2]. Under ideal growth conditions, microalgae have the potential of synthesizing neutral lipids in the form of triacylglycerol and can be induced in many species under various stress factors [3]. Although the increased lipid accumulation under stress conditions lowers the cell growth, resulting a significant decrease in the biomass productivity. Reports on nitrogen-starved condition in some species such as *Chlorella* and *Nannochloropsis* species

Electronic supplementary material The online version of this article (doi:10.1007/s13399-016-0198-6) contains supplementary material, which is available to authorized users.

✉ K. Mohanty
kmohanty@iitg.ernet.in

✉ Vaibhav V. Goud
vvgoud@iitg.ernet.in

[1] Centre for Energy, Indian Institute of Technology Guwahati, Assam 781039, India

[2] Department of Chemical Engineering, Indian Institute of Technology Guwahati, Assam 781039, India

recorded up to two- to fourfold increase in the lipid content [3–5]. Therefore, such enhancement could be incorporated to the mass cultivation for increased oil recovery for biofuel applications. Moreover, a selection of ideal strain is also crucial to algal biofuel research that provides high lipid and biomass yield.

An effective and rapid analytical technique is in a high note for lipid and fatty acid analysis. Recently, Fourier transform infrared spectroscopy (FTIR) has emerged as an attractive alternative technique due to its inexpensive and rapid nature [6]. FTIR is often coupled with chemometric methods for quantitative analysis of certain plant oils [7]. Nowadays, the importance of chemometric techniques in the study of edible fats and oils are often observed for the confirmation study [8]. The chemometric technique like multivariate calibrations extracts information of the FTIR spectrum and its response to the concentration of analyte(s) [7]. And most techniques used for the quantitative assessment are namely the principal component regression (PCR), partial least squares (PLS) regression, multivariate curve resolution [9], and the independent component analysis (ICA) method [7, 10, 11].

The present study was carried out to analyze the FTIR spectrum of *Chloromonas* species (ADIITEC-III) oil sample in response to a different nitrogen source using the chemometric techniques of cluster analysis and multivariate calibrations. The technique was basically used to comprehend the large and complex data set of vibrational frequencies (wave numbers) into a simplified manner. The *Chloromonas* species (ADIITEC-III) was isolated from locally adapted algal diversity and showed its potentiality in terms of its adaptability, biomass production, and lipid content in our preliminary trials. Furthermore, the data presented herewith are reported the first time for the strain and could be helpful for future investigation on its potential applications.

2 Methods

2.1 Microalgae strain and cultivation conditions

The *Chloromonas* species (ADIITEC-III) was isolated from the water sample collected from the native freshwater reservoir of Amingaon, Kamrup district, Assam, India. The microalgae was cultivated in an artificial medium and consist of following components (per liter): $NaNO_3$ (1.5), $K_2HPO_4 \cdot 3H_2O$ (0.04), $KH_2PO_4 \cdot 3H_2O$ (0.2), EDTA (0.0005), Fe ammonium citrate (0.005), citric acid (0.005), Na_2CO_3 (0.02), and 1 ml of trace metal composed of H_3BO_3 (2.85 g), $MnCl_2 \cdot 4H_2O$ (1.8 g), $ZnSO_4 \cdot 7H_2O$ (0.02 g), $CuSO_4.5H_2O$ (0.08 g), $CoCl_2 \cdot 6H_2O$ (0.08 g), and $Na_2MoO_4 \cdot 2H_2O$ (0.05 g) in 1000 ml double-distilled water. The pH of the medium was adjusted to 7.5 with an either 1N HCl or 1N KOH solution prior to autoclaving. The flasks were incubated at 25 ± 1 °C temperature with intermittent illumination (16:8 h light and dark cycle) of 35 μmol photons m^{-2} day^{-1}.

For the study of different nitrogen sources, the artificial medium was supplemented with potassium nitrate (KN), sodium nitrate (Na), urea (U), and ammonium nitrate (AN) at the same concentration of 1.5 mM, respectively. The cultivation conditions are kept the same as mentioned above.

2.2 Determination of growth and biomass estimation

The microalgae cell density was determined with the help of a Neubour hemocytometer by counting the cell numbers. Specific growth rates were calculated using the equation given by Levasseur et al. (1993) [12]:

$$\mu = \frac{[Ln(N_2/N1]}{t2-t1} \quad (1)$$

Where, N_1 and N_2 = biomass at time (t_1) and time (t_2), respectively.

The doubling time (T_2) was calculated using the equation:

$$T_2 = \frac{0.6931}{\mu} \quad (2)$$

Biomass determination was carried out gravimetrically by estimating the dry algal cells harvested by filtering a definite volume of culture suspension through a pre-weighed Whatman filters (GF/C filter paper). The difference between the final and initial weight of the GF/C filter paper denotes a dry weight of the sample and was expressed in gram dry weight per liter (g L^{-1}).

2.3 Lipid extraction

The lipid content was extracted using *n*-hexane (100 ml) in a Soxhlet apparatus at 50 °C under reflux condition for 16 h. Approximately, 1 g of grinded dry cells were used to extract the lipid in three triplicates. The excess solvent was recovered using rotary evaporator at 50 °C under reduced pressure and the extracted total lipid was measured gravimetrically and expressed as percent dry cell weight (% DCW) [13].

2.4 FTIR analysis

The functional group of oil sample was analyzed using Fourier transform infrared spectroscopy (IR Affinity-1 Shimadzu). Prior to analysis, the sample was homogenized with KBr. A normal scanning range of 400–4000 cm^{-1} was employed for 30 repeated scans at a spectral resolution of 4 cm^{-1} with a pair of KBr crystals in thin film. The spectra were recorded in transmittance mode.

2.5 Multivariate analysis of FTIR spectra

For multivariate data analysis, two FTIR spectral regions were selected, i.e., a lipid acyl region (3000–2800 cm^{-1}) and bimolecular fingerprint region (1800–1000 cm^{-1}). The software SAS JMP, version 10, and XLSTAT 2014 for Windows were used for principal component analysis (PCA), hierarchical clustering analysis (HCA), and multidimensional scaling (MDS).

3 Results and discussion

3.1 Effect of different nitrogen sources on growth and lipid accumulation

Under stated growth conditions, *Chloromonas* species (ADIITEC-III) was cultivated over 10 days for standardizing the appropriate nitrogen source. The growth curve (Fig. 1) for four different nitrogen sources revealed an initial lag phase from the day of inoculation. Among the treated nitrogen sources, potassium nitrate and sodium nitrate showed almost a similar trend of growth with maximum specific growth rate (μmax) of 0.23 d^{-1} and 0.2 d^{-1}, respectively. The biomass with sodium nitrate as a nitrogen source was significantly higher than the other nitrogen sources, which was approximately 0.39 ± 0.01 g L^{-1} (dry mass) at the terminal day (10 days) of culture duration (Table 1). In contrast, potassium nitrate was not much responsive for algal lipid yield (28.40 ± 2.85 %) and invariably was similar to that of ammonium nitrate (30.2 ± 0.87 %). However, algae fed with urea showed slow growth, but the recovery of lipid was more, i.e., 37.35 ± 0.32 %. The findings clearly indicated that nitrogen in the nitrate forms (potassium and sodium nitrate) favored the algal growth over ammonium nitrate. Moreover, it is also suggested that the nitrate and ammonium uptake interaction inhibits the microalgae cells in nitrate uptake, as the product obtained through ammonium assimilation causes a rapid and reversible inactivation of nitrate transport [14]. Several studies on nitrogen supplementation for algal growth, biomass, and lipid production have been reported in many species such as *Porphyridium purpureum* [15], *Scenedesmus dimorphous* [16], *Tetraselmis suecia*, *Skeletonema costatum*, and *Thalassiosira pseudonana* [1]. The study also supports the nitrogen source supplied in any form to promote growth and lipid accumulation in microalgae.

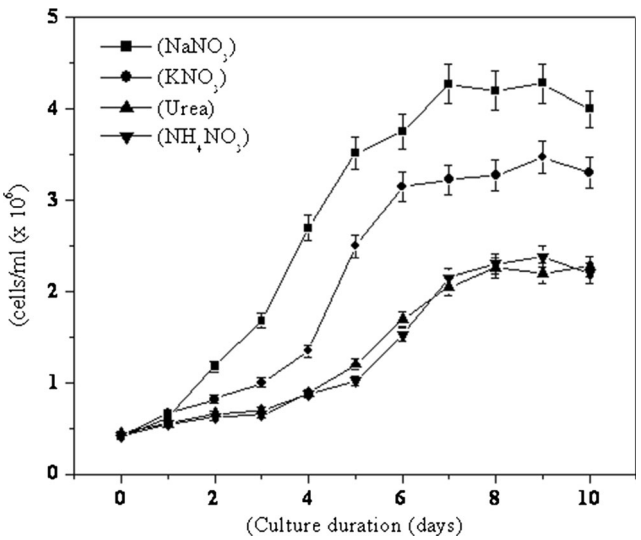

Fig. 1 Growth curve of *Chloromonas* species ADIITEC-III in different nitrogen sources

3.2 FTIR analysis

The FTIR spectra of algal lipid extracts for different nitrogen sources are shown in Fig. 2. The mid-infrared region 3500–1000 cm^{-1} of spectra illustrates the distinct absorption bands which is assigned and characterized based on biochemical standards and published literature [3, 17]. The band region 3000–2800 cm^{-1} was attributed from the aliphatic C–H stretching vibration and C–H bending region 1500–1300 cm^{-1}; meanwhile, the intense absorption bands at 1746–1654 cm^{-1} corresponds to the C=O ester [6]. The appearance of FTIR spectrum of treated lipid extracts illustrated the distinct IR bands in the aforementioned regions which suggest the distinct nature of lipid existence. The near compositional similarities and dissimilarities of the FTIR spectrum was served as frequency region selection for classification and quantification of lipid recovered from the treatment. Herein, to evaluate the possible spectral variations among the FTIR spectrum of the lipid extracts, two key spectral regions were chosen: the hydrocarbon region 3000–2800 cm^{-1} and the bimolecular region 1800–1000 cm^{-1}. Therefore, apparent distinctions among the treatments in the selected regions are further explained by multivariate analysis.

3.2.1 Principal component analysis

Under different nitrogen sources, the observed variations in IR response are due to the chemical heterogeneity which is further subjected to PCA for data comparison. The PCA was performed in the selected spectral region which helps in reproducing the most prominent variation pattern in the data. The absorption bands observed at 3000–2800 and 1800–1000 cm^{-1} were used in this study, since these spectral ranges are dominated by the lipid acyl chain absorption and biomolecular fingerprint, respectively.

At first, analysis was performed in the region 3000–2800 cm^{-1}, the PCA score plots obtained by analyzing the measured IR spectrum represented significant

Table 1 Comparison of specific growth, doubling time, biomass concentration, and total lipid content of *Chloromonas species* (ADIITEC-III) in different nitrogen sources

Nitrogen source	Specific growth	Doubling time	Biomass concentration (g L^{-1})	Lipid (%)
$NaNO_3$ (Na)	0.23	3.01	0.39 ± 0.01	35.86 ± 2.3
KNO_3 (KN)	0.20	3.38	0.31 ± 0.02	28.40 ± 2.85
Urea (U)	0.16	4.27	0.23 ± 0.04	37.35 ± 0.32
NH_4NO_3 (AN)	0.17	4.22	0.29 ± 0.04	30.2 ± 0.87

contribution of the studied parameters by this method. From Fig. 3a and b, it can be seen that PC1 and PC2 contributed to the majority of total variations which was equivalent to 98.79 % (PC1 and PC2 accounted for 92.3 and 6.49 %, respectively) and are expected to be useful for disclosing the data correlations. As can be seen in the figure, variables are clearly resolved by the two PCs which explain the correlations near the periphery of the circle. It also exhibits the difference between the variables represented by ammonium nitrate, and urea is separated by the first PC factor from sodium and potassium nitrate. The scatter plot observed in Fig. 3b indicates a distinct group of spectral data due to the similar chemical structure. Nevertheless, the dissimilar chemical nature contributed to the spectral profiles creates the spread of variation along the two principal axes. Moreover, the first principal component (PC1) accounted the largest contributions which might be due to the CH_2 stretching modes at around 2850 and 2922 cm^{-1}, followed by the CH_3 component at 2960 cm^{-1}. As illustrated in Table S1 (Supporting Information) among the different variables, a maximum variance of 26.882 % was contributed by urea in PC1, and ammonium nitrate contributes a maximum variance of 60.197 % in PC2. Therefore, the obtained result confirms the correlations of original variables and the cumulated percentage of variance of each variable explained by PC1 and PC2.

To better evaluate the lipid changes in different treatments, PCA has been extended to the spectral range between 1800 and 1000 cm^{-1}, since this spectral range is the biomolecular fingerprint region. In addition, the multidimensional scaling of the region 1800 and 1000 cm^{-1} also suggests that the calculated distances were much larger than the analysis performed at the higher wave numbers (Table S2, Supporting Information). In this region, the complexities of IR responses due to the absorption of lipids and the biomolecules are better explained by the PC analysis. Interestingly, as reported in the loading plot of Fig. 4b, PC1 contributed 87.24 % of total variations, whereas PC2 contributed to 7.62 %. In this region (i.e., 1800–1000 cm^{-1}) the score plot also shows that potassium nitrate and urea are separated by the first PC factor from sodium nitrate and ammonium nitrate (Fig. 4b).

From Fig. 4a, it was noticed that the two-dimensional score plots (PCA) obtained by analyzing the IR spectra of different

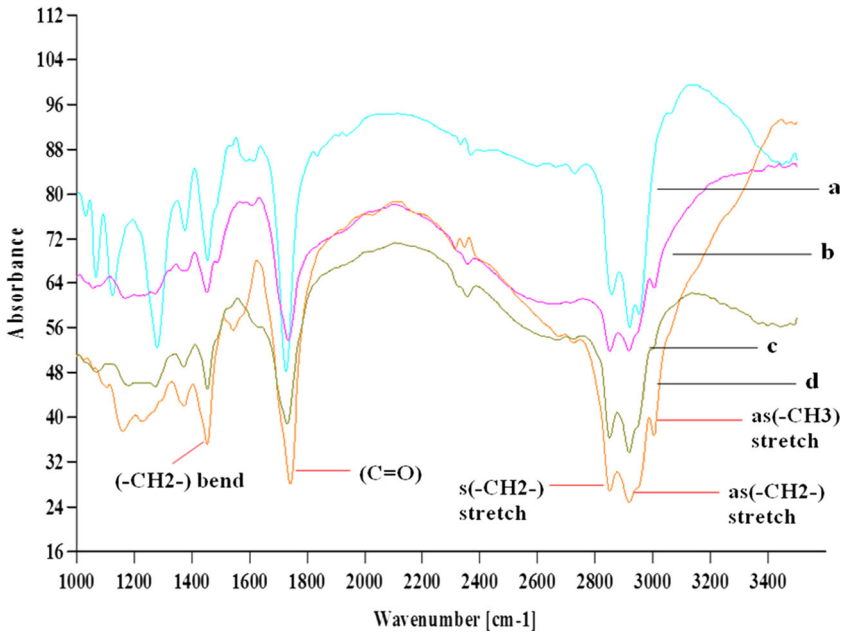

Fig. 2 FTIR spectra of lipid extracts scanned at mid-infrared region (3500–1000 cm^{-1}). FTIR spectrum showing the characteristic lipid hydrocarbon bands apparent in the spectra of (*a*) KNO_3, (*b*) NH_4NO_3, (*c*) Urea, and (*d*) $NaNO_3$

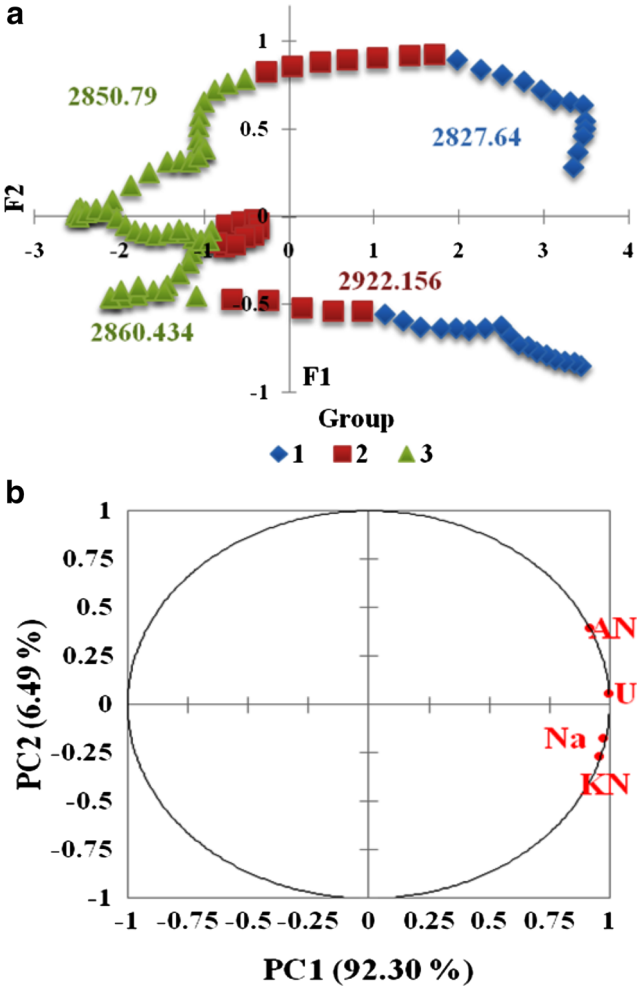

Fig. 3 Principal component analysis of spectral region (3000–2800 cm^{-1}) of the treatments. **a** The 2D scatter plot of PC1 × PC2 showing variance contribution and **b** the loading plot showing the linear coefficients

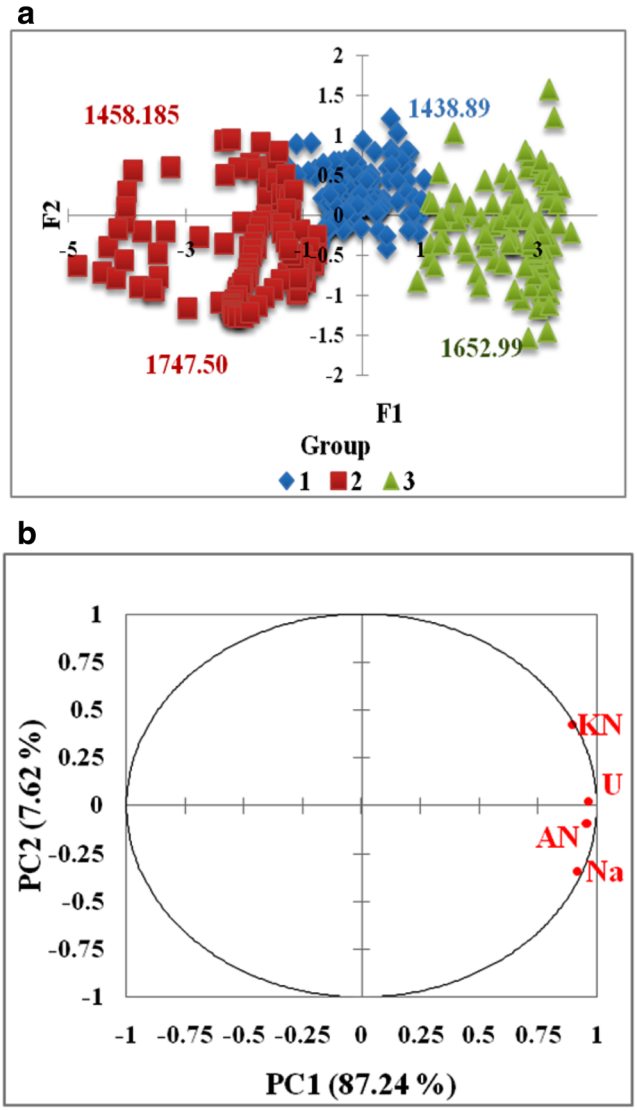

Fig. 4 Principal component analysis of spectral region (1800–1000 cm^{-1}) of the treatments. **a** The 2D scatter plot of PC1 × PC2 showing variance contribution and **b** the loading plot showing the linear coefficients

treatments showed that PC1 was mainly governed by C=O ester band and C=C stretching. Furthermore, multidimensional scaling (MDS) for both the region, i.e., 3000–2800 and 1800–1000 cm^{-1} of FTIR spectra showed significant variation in studied nitrogen sources. The Shephard diagram (Fig. 5a) of region 1800–1000 cm^{-1} with the stress value (Kruskal's stress) of 0.011 showed a good fit of the model. Whereas, the Shephard diagram (Fig. 5b) of region 3000–2800 cm^{-1} showed the stress value (Kruskal's stress) of 8.251 E-4.

The data obtained from MDS analysis provide minimum dissimilarity of 107.10 between urea and sodium nitrate in the region 3000–2800 cm^{-1} (Table S3, Supporting Information). Similarly, the minimum dissimilarity of 132.13 was also observed between urea and sodium nitrate at the spectral region 1800–1000 cm^{-1} (Table S4, Supporting Information). Overall, MDS analysis shows close proximity between urea and sodium nitrate and discriminates potassium nitrate in both the spectral regions.

3.2.2 Cluster analysis

Hierarchical clustering analysis (HCA) was performed using the ward method between hydrocarbon region 3000–2800 cm^{-1} (Fig. 6a) and biomolecular fingerprint region 1800–1000 cm^{-1} (Fig. 6b). The results of HCA for the spectral range between 3000 and 2800 cm^{-1} are displayed as dendrograms to understand the correlation between each pair of variables. Figure 6a indicated three main clusters of variables based on its scaling distance. The first cluster formed by ammonium nitrate alone was found to be distantly connected to the third cluster. The first cluster gradually connects to the second cluster formed by potassium nitrate. The cluster observed at the lowest distance level was formed by closely

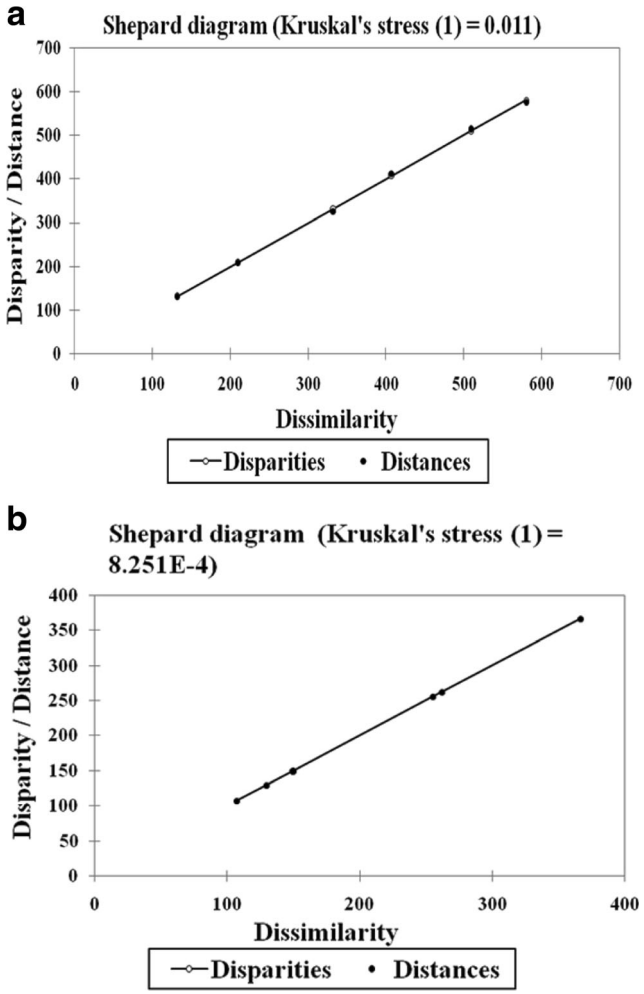

Fig. 5 The multidimensional scaling of FTIR spectrum spectral region (3000–2800 cm^{-1}). **a** The calculated stress value (Kruskal's stress (1) = 0.011) in the Shephard diagram of region 1800–1000 cm^{-1}. **b** The calculated stress value (Kruskal's stress (1) = 8.251 E-4) of region 3000–2800 cm^{-1}

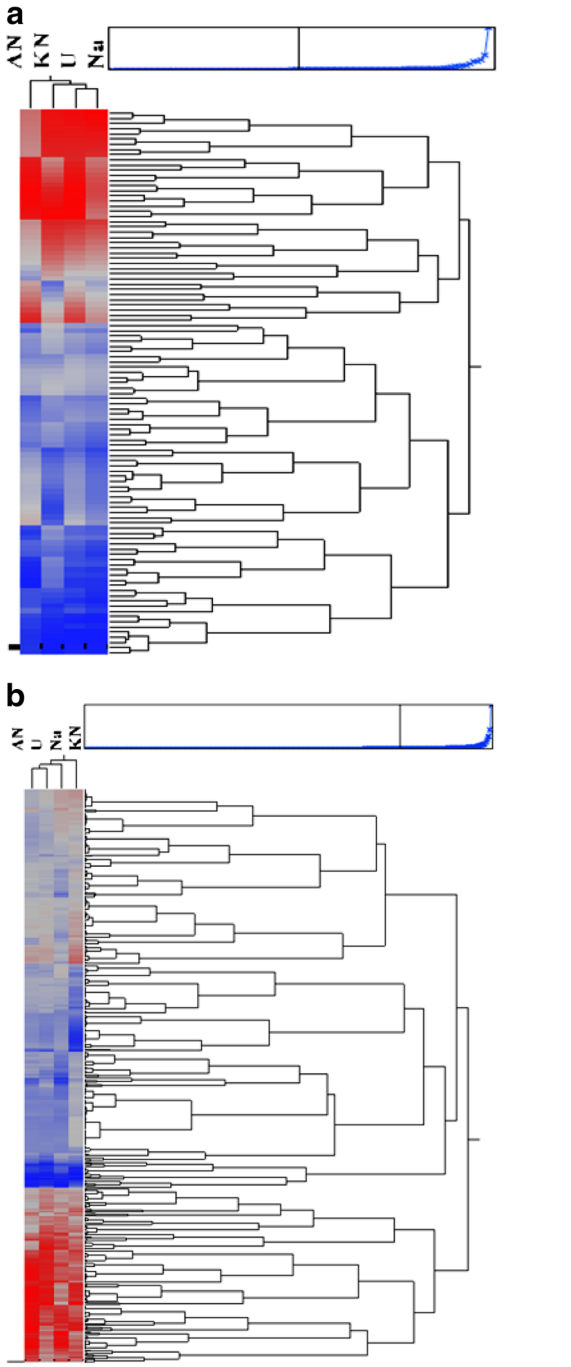

Fig. 6 **a** Hierarchical clustering dendrograms for the spectra (3000–2800 cm^{-1}). **b** Dendrograms for spectra in the spectral regions between 1800 and 1000 cm^{-1}

similar variables, i.e., urea and sodium nitrate. Interestingly, the dendrogram derived from the HCA of the bimolecular fingerprint region (Fig. 6b) was distinctively different from the dendrogram of the spectral region between 3000 and 2800 cm^{-1}. In this case, the first main cluster formed by ammonium nitrate and the lowest distance level formed by urea were closely similar and gradually connected to sodium nitrate. The third cluster formed by potassium nitrate was observed alone and distantly connected to the first main cluster.

4 Conclusion

The lipid recovered from *Chloromonas* species (ADIITEC-III) in different nitrogen sources was further characterized in order to understand the quantitative response of nitrogen towards the lipid accumulation. From the perspective of maximum lipid yield, the different nitrogen sources exhibit in following preferential order: urea > sodium nitrate > ammonium nitrate > potassium nitrate. The FTIR spectrum coupled with multivariate analysis demonstrated the applicability of the selected spectral regions of the treatments. The technique could act as a useful support for rapid industrial-based process analysis to ensure the authenticity of the product.

Acknowledgments The work reported in this article was financially supported by a research grant (vide grant no. 22 (0600)/12/EMR-II) received from the Council for Scientific and Industrial Research (CSIR), Government of India.

References

1. Arumugam M, Agarwal A, Arya MC, Ahmed Z (2013) Influence of nitrogen sources on biomass productivity of microalgae *Scenedesmus bijugatus*. Bioresour Technol 131:246–249
2. Li YQ, Horsman M, Wang B, Wu N, Lan CQ (2008) Effects of nitrogen sources on cell growth and lipid accumulation of green alga *Neochloris oleoabundans*. Appl Microbiol Biotechnol 81: 629–636
3. Dean AP, Sigee DC, Estrada B, Pittman JK (2010) Using FTIR spectroscopy for rapid determination of lipid accumulation in response to nitrogen limitation in freshwater microalgae. Bioresour Technol 101:4499–4507
4. Illman AM, Scragg AH, Shales SW (2000) Increase in *Chlorella* strains calorific values when grown in low nitrogen medium. Enzym Microb Technol 27:631–635
5. Rodolfi L, Zittelli GC, Bassi N, Padovani G, Biondi N, Bonini G, Tredici MR (2009) Microalgae for oil: strain selection, induction of lipid synthesis and outdoor mass cultivation in a low-cost photobioreactor. Biotechnol Bioeng 102:100–112
6. Talukdar J, Kalita MC, Goswami BC, Hong DD, Das HC (2014) Liquid hydrocarbon production potential of a novel strain of the microalga *Botryococcus braunii*: assessing the reliability of in situ hydrocarbon recovery by wet process solvent. Energy Fuel 28(6): 3747–3758
7. Rohman A, Man YBC (2012) The chemometrics approach applied to FTIR spectral data for the analysis of rice bran oil in extra virgin olive oil. Chemom Intell Lab 110:129–134
8. Arvanitoyannis IS, Vlachos A (2007) Implementation of physicochemical and sensory analysis in conjunction with multivariate analysis towards assessing olive oil authentication/adulteration. Crit Rev Food Sci Nutr 47:441–498
9. Vlachos N, Skopelitis Y, Psaroudaki M, Konstantinidou V, Chatzilazarou A, Tegou E (2006) Applications of Fourier transform-infrared spectroscopy to edible oils. Anal Chim Acta 573–574:459–465
10. Rohman A, Man YBC (2010) Fourier transform infrared (FTIR) spectroscopy for analysis of extra virgin olive oil adulterated with palm oil. Food Res Int 43:886–892
11. Luca MD, Oliverio F, Loele G, Ragno G (2009) Multivariate calibration techniques applied to derivative spectroscopy data for analysis of pharmaceutical mixtures. Chemom Intell Lab Syst 96:14–21
12. Levasseur M, Thompson PA, Harrison PJ (1993) Physiological acclimation of marine phytoplankton to different nitrogen sources. J Phycol 29:587–595
13. Talukdar J, Kalita MC, Goswami BC (2013) Characterization of the biofuel potential of a newly isolated strain of the microalga *Botryococcus braunii* Kützing from Assam, India. Bioresour Technol 149:268–275
14. Flynn KJ (1991) Algal carbon-nitrogen metabolism: a biochemical basis for modeling the interactions between nitrate and ammonium uptake. J Plankton Res 13:373–387
15. Becker EW (1994) Microalgae: biotechnology and microbiology. Cambridge University Press, Cambridge
16. Benider A, Tahiri M, Belkoura M, Dauta A (2001) Interacting effect of heliothermic factors on the growth rate of 3 *Scenedesmus* species. Int J Limnol 37:257–266
17. Stehfest K, Toepel J, Wilhelm C (2005) The application of micro-FTIR spectroscopy to analyze nutrient stress-related changes in biomass composition of phytoplankton algae. Plant Physiol Biochem 43:717–726